The Catalytic Machinery of Chondroitinase ABC I Utilizes a Calcium Coordination Strategy to Optimally Process Dermatan Sulfate†

Vikas Prabhakar, Ishan Capila, Rahul Raman, Aravind Srinivasan, Carlos J. Bosques, Kevin Pojasek, Michael A. Wrick, and Ram Sasisekharan*

Division of Biological Engineering, Massachusetts Institute of Technology, Cambridge, Massachusetts 02139

Received March 18, 2006; Revised Manuscript Received June 22, 2006

ABSTRACT: The chondroitinases are bacterial lyases that specifically cleave chondroitin sulfate and/or dermatan sulfate glycosaminoglycans. One of these enzymes, chondroitinase ABC I from *Proteus vulgaris*, has the broadest substrate specificity and has been widely used to depolymerize these glycosaminoglycans. Biochemical and structural studies to investigate the active site of chondroitinase ABC I have provided important insights into the catalytic amino acids. In this study, we demonstrate that calcium, a divalent ion, preferentially increases the activity of chondroitinase ABC I toward dermatan versus chondroitin substrates in a concentration-dependent manner. Through biochemical and biophysical investigations, we have established that chondroitinase ABC I binds calcium. Experiments using terbium, a fluorescent calcium analogue, confirm the specificity of this interaction. On the basis of theoretical structural models of the enzyme−substrate complexes, specific amino acids that could potentially play a role in calcium coordination were identified. These amino acids were investigated through site-directed mutagenesis studies and kinetic assays to identify possible mechanisms for calcium-mediated processing of the dermatan substrate in the active site of the enzyme.

Chondroitin sulfate (CS[1]) and dermatan sulfate (DS) are acidic polysaccharides of the glycosaminoglycan (GAG) family that serve important functions in a variety of biological processes, including neuronal development, coagulation, inflammation, cellular trafficking, cellular proliferation, and oncogenesis (*1*−*8*). Both CS and DS comprise a repeat disaccharide unit of β-D-*N*-acetyl galactosamine (GalNAc) linked 1 → 4 to uronic acid. These basic disaccharide units are linked 1 → 3 to form polysaccharide chains. The uronic acid moiety of CS exists as the β-D-glucuronic acid (GlcA) epimer, and in DS as the α-L-iduronic acid (IdoA) epimer. The polysaccharide backbone may be modified by sulfation at the 4-*O* and 6-*O* position of the GalNAc as well as the 2-*O* position of the uronic acid (*9*).

The chemical complexity of these GAGs has hampered a refined comprehension of their structure−function relationships with other biomolecules. Thus, defining the biological roles of GAGs is often difficult (*10*). The specific sequence of chemical modifications on GAG chains imparts a potential for interaction with other biological agents, including growth factors, cytokines, and other signal transducers (*9*). Even more, specific sequences within the oligosaccharide chain have been shown to be activating and others to be inhibitory, with regard to specific biological processes (*11*). Decoding the GAG sequence is, therefore, critical in understanding structure−function relationships.

The development of complementary biochemical tools that cleave GAGs in a sequence-specific fashion has enabled progress in the polysaccharide sequencing field. Many microorganisms express GAG-degrading enzymes for the purpose of facile invasion of host tissue and to acquire nutrition from decaying animal carcasses. A number of these enzymes have been cloned, recombinantly expressed, and characterized in terms of their substrate specificity and catalytic activity. These include heparinases I (*12*), II (*13*, *14*), and III (*15*) and chondroitinases AC and B (*16*−*19*) (cAC and cB, respectively) from *Pedobacter heparinus* (formerly known as *Flavobacterium heparinum*). These enzymes are lyases that cleave at the glycosidic linkage between the hexosamine and the uronic acid. The recombinant expression and biochemical characterization of these enzymes has enabled their application in polysaccharide sequencing methodologies (*10*), the investigation of structure−function relationships in tumorigenesis (*20*), and other industrial applications (*21*).

Continuing our efforts to develop GAG-degrading enzymes as biochemical tools, we recently cloned and recombinantly expressed chondroitinase ABC I, a broad substrate specific enzyme from *Proteus vulgaris* (*22*). By constructing theoretical models of enzyme−substrate complexes using the structure of cABC I (*22*), we investigated the putative active

† This work was supported by National Institutes of Health Grant GM57073. The authors thank the Multiuser Facility for the Study of Complex Macromolecular Systems (NSF-0070319 and NIH-GM68762) for access to instrumentation. V.P. was funded through the National Institutes of Health Biotechnology Training Grant (5-T32-GM08334) and a Dupont Fellowship (Massachusetts Institute of Technology). C.B. was funded through the NIH/NIEHS Training Grant in Environmental Toxicology (5-T32-ES0720).

* Corresponding author. Tel: 617-258-9494. Fax: 617-258-9409. E-mail: rams@mit.edu.

[1] Abbreviations: CS, chondroitin sulfate; DS, dermatan sulfate; GAG, glycosaminoglycan; GalNAc, β-D-*N*-acetyl galactosamine; cABC I, chondroitinase ABC I; cAC, chondroitinase AC; cB, chondroitinase B; C6S, chondroitin-6-sulfate; CD, circular dichroism; IdoA, iduronic acid; GlcA, glucuronic acid; C4S, chondrotin-4-sulfate.

10.1021/bi0605484 CCC: $33.50
Published on Web 08/25/2006

site amino acids via site-directed mutagenesis. These preliminary studies into cABC I's active site topology indicated potential differences in the processing of CS and DS substrates by this enzyme. These putative differences were attributed to the different orientations of the *C*-5 proton of the uronic acid relative to the cleavable glycosidic bond, depending on the epimerization state (*23*, *24*).

In this study, we investigated in great detail the differences in the processing of CS and DS substrates by cABC I. We specifically examined the role of divalent cations such as calcium in catalysis. Previously, it has been observed that calcium is required for the optimal activity of several polysaccharide-degrading enzymes. These include heparinase I (*25*, *26*) and chondroitinase B (*27*) from *Pedobacter heparinus*, and pectate lyase C (*28*) from *Erwinia chrysanthemi*. In all these enzymes, calcium has played an important role in catalysis. The involvement of calcium could be explained on the basis of several scenarios. The binding of calcium to the enzyme facilitates substrate cleavage and, thus, enhances its catalytic activity. Alternatively, a specific interaction of calcium with the substrate (*29*) enables a favorable conformation that can be optimally processed by the enzyme.

In an effort to examine whether divalent ions play an important role in cABC I activity, we undertook a series of experiments to determine whether cABC I binds divalent ions and, if so, at which sites this interaction might take place, and how this might affect enzyme activity and substrate processing. In this study, we indeed find that cABC I binds calcium. Through fluorescence spectroscopy studies and the development of site-directed mutants of the enzyme's putative calcium binding site, we characterize cABC I's selective requirement of calcium for the optimal processing of one of its substrates, DS.

EXPERIMENTAL PROCEDURES

Materials. Porcine intestinal mucosa DS (average MW 35,000 g/mol) and shark cartilage chondroitin-6-sulfate (C6S, average MW 50 000 g/mol) were purchased from Sigma. Oligonucleotides were purchased from Invitrogen. The QuikChange Site-Directed Mutagenesis Kit was purchased from Stratagene. The QIAprep Spin Miniprep Kit was purchased from Qiagen. Protein concentration was measured using the Bio-Rad Laboratories Bradford assay kit. Chelex resin was purchased from Bio-Rad. $TbCl_3$ was purchased from Aldrich. All other materials are from common sources or are as noted under Experimental Procedures.

Site-Directed Mutagenesis of Chondroitinase ABC I. The development of recombinant cABC I and the methods used to produce cABC I mutants are previously described (*23*). The primer sequences for each of the mutants are listed below. The Asp439Ala mutant primers have the sequences 5′- GAT ATG AAA GTA AGT GCT **GCT** AGC TCT GAT CTA G-3′ and 5′- C TAG ATC AGA GCT AGC AGC ACT TAC TTT CAT ATC-3′. The Asp442Ala mutant primers have the sequences 5′- GT GCT GAT AGC TCT **GCT** CTA GAT TAT TTC AAT ACC-3′ and 5′- GGT ATT GAA ATA ATC TAG AGC AGA GCT ATC AGC AC-3′. The Asp444Ala mutant primers have the sequences 5′- AGC TCT GAT CTA **GCT** TAT TTC AAT ACC TTA TCT CGC C-3′ and 5′- G GCG AGA TAA GGT ATT GAA ATA AGC TAG ATC AGA GCT-3′. The Asp490Ala mutant primers have the sequences 5′- CCG GGT GGT AAA **GCT** GGT TTA CGC CCT-3′ and 5′- AGG GCG TAA ACC AGC TTT ACC ACC CGG-3′. The Tyr392Ala mutant primers have the sequences 5′- CC CAT CAC TGG GGA **TTC** AGT TCT CGT TGG TGG-3′ and 5′- CCA CCA ACG AGA ACT GAA TCC CCA GTG ATG GG-3′. Plasmids were prepared using a miniprep kit, and each clone was sequenced to confirm the incorporation of the desired mutation.

Protein Expression and Purification. Recombinant cABC I and the site-directed mutants were expressed and purified as previously described (*24*). Protein purity was assessed by SDS−polyacrylamide gel electrophoresis analysis using precast Invitrogen NuPAGE 12% Bis-Tris gels, the XCell SureLock Mini-Cell, and Simply Blue SafeStain. Protein content was assessed by standard methods using a Bradford assay kit with bovine serum albumin (Sigma) as a standard. In order to ensure that there were no structural perturbations in the mutant enzymes when compared to recombinant cABC I, a structural characterization was undertaken using circular dichroism (CD). Recombinant proteins were concentrated and buffer exchanged into 50 mM sodium phosphate at pH 8.0 using Centricon 10 filters (Millipore). Protein content was assessed using the Bradford assay. CD spectra were recorded at 25 °C on an Aviv 202 CD spectrophotometer using Quartz cuvettes with an optical path length of 0.1 cm. Scans were collected between 195 and 280 nm with a 1.0-nm bandwidth and a scan rate of 1 nm/min. Three scans were averaged for each protein. All spectra were collected using a protein concentration of 0.2 mg/mL.

Fluorescence Spectrometry. For terbium titrations of cABC I, aliquots of a terbium stock solution in 10 mM MOPS and 0.1 M KCl at pH 7.0 were added to a solution containing 5 μM cABC I. The concentration of the terbium solution was determined by EDTA titration in the presence of a xylenol orange indicator (*26*). To ensure accurate readings, all solutions (except the terbium stock) were run through a chelating column (Chelex resin) to remove trace contaminants. After terbium addition, the sample was mixed and allowed to come to equilibrium for 15 min. Fluorescence measurements were recorded on a Cary Eclipse fluorescence spectrophotometer. The geometry of fluorescence detection was 90°. All experiments employed a quartz cell with a 1.0-cm path length. The excitation wavelength was either 488 nm (direct excitation of terbium) or 280 nm (excitation of proximal tyrosine residues), and the emission wavelength was 545 nm. Experiments involving divalent ion competition titrations of cABC I were also performed. To a solution of cABC I and 6 mM terbium, a calcium solution was added. After addition, the solution was mixed and allowed to stand for 15 min before being measured.

Effect of Divalent Ions on Recombinant cABC Activity. For these studies, C6S and DS were dissolved at a 1 mg/mL concentration in 50 mM Tris at pH 8.0 (no salt) containing a fixed concentration (10 mM) of different divalent ion salts ($CaCl_2$, $MgSO_4$, $MnCl_2$, and ZnCl2). Recombinant cABC I (0.2 μg) was added to each of these solutions, and the activity of the enzyme was assessed on the basis of the change in absorbance at 232 nm (A_{232}/minute). These experiments were carried out on a SpectraMax 190 (Molecular Devices) using a 96-well quartz plate as previously described (*23*). The temperature was set at 37 °C for these experiments, and

enzyme activity was calculated on the basis of the initial rate of product formation.

Docking Models. The cocrystal structures of cAC with C4S and DS were superimposed on the cABC I crystal structure on the basis of the structural alignment between these enzymes (obtained using the SARF2 program). The superimposition (452 CA atoms with a rmsd of 2.2 Å) provided the starting structures for the cABC I−substrate complexes. The coordinates of C4S (GlcA−GalNAc4S)$_2$ and DS (IdoA−GalNAc4S)$_2$ tetrasaccharides were available from the two cAC cocrystal structures. In the case of C4S, the C5 proton of GlcA and the glycosidic oxygen of the cleavable linkage were facing the active site. However, in the case of DS, the C5 proton of IdoA and the glycosidic oxygen of the cleavable linkage were facing opposite directions. Thus, two different initial substrate conformations for DS were generated by sampling the conformational space of the cleavable glycosidic linkage. In the first conformation, the C5 proton of IdoA was facing the active site to facilitate cleavage. In the second conformation, the carboxylate group of the IdoA was facing the other amino acids that constituted the putative calcium binding site. The glycosidic oxygen atom in the second conformation was facing the active site to facilitate protonation of the leaving group.

These starting structures of the enzyme substrate structural complexes were further optimized using energy minimization. The AMBER force field modified for carbohydrates was further modified to include *O*-sulfate and sulfamate groups. This modified AMBER force field was used to assign the potentials for both the enzyme as well as the tetrasaccharide substrates. A subset of the enzyme coordinates around the active site groove was defined to include all of the putative active site amino acids and several additional amino acids that could potentially be involved in catalytic activity. The enzyme−substrate complex was subject to minimization, first without charges and then with charges using 500 steps of steepest descent and 500 steps of conjugate gradient methods. Most of the protein was fixed, and only the amino acids that were a part of the active site subset were allowed to move during the minimization. The final rms derivatives of the energies were below 0.1. The ring conformation of the monosaccharides was not distorted by the minimization procedure. The Viewer and Discover modules of InsightII (release 2000.1, Accelrys, San Diego, CA) were used for the orientation of the substrate and the energy minimization, respectively.

Chondroitinase ABC I Activity Assessments. A kinetic analysis of cABC I employed our semi high-throughput spectrophotometric approach and is essentially as that previously described (*23*). Briefly, 1 μL of 0.2 μg/μL cABC I was added to 249 μL of a solution containing DS or C6S in 50 mM Tris-HCl, 50 mM sodium acetate, and 10 mM calcium chloride at pH 8.0. Enzyme concentration (8 nM) was chosen so as to keep the substrate in excess. Each well contained different substrate concentrations ranging from 0.1 to 5 mg/mL. Product formation was monitored by measuring the absorbance at 232 nm every 2 s for 2 min. To evaluate the kinetic data, the initial reaction rate (v_o) was first determined from the value of the slope from the plot of product formation as a function of time over 20 s. The values of V_{max} and K_m were extracted from the slope and *y*-intercept of the Hanes plot generated by monitoring the product formation. A molar absorptivity coefficient (ϵ) for the product of the enzymatic reaction of 3800 $M^{-1}\cdot cm^{-1}$ was used. The calculated value for the path length of the well using a 250 μL volume for the reaction was 0.904 cm. The analyses were performed in triplicate.

Table 1: Specific Activity of Chondroitinase ABC I Acting on Chondroitin-6-sulfate and Dermatan Sulfate in the Presence of Divalent Ions

divalent ion[a]	specific activity (Units/mg protein)
substrate: chondroitin-6-sulfate	
Tris pH 8	169.7 ± 9.7
Ca^{2+}	158.2 ± 10.5
Mn^{2+}	129.3 ± 6.2
Mg^{2+}	200.7 ± 17.4
Zn^{2+}	19.1 ± 3.2
substrate: dermatan sulfate	
Tris pH 8	8.9 ± 3.3
Ca^{2+}	231.3 ± 8.2
Mn^{2+}	12.8 ± 7.5
Mg^{2+}	262.8 ± 7.2
Zn^{2+}	20.4 ± 1.7

[a] Divalent ions (chloride or sulfate salts) are added to the basic buffer of 50 mM Tris at pH 8.0 (no additional salt) at a concentration of 10 mM. Recombinant cABC I (0.2 μg) was added to each of these solutions. The absorbance at 232 nm was monitored in order to measure enzyme activity. Specific activity is reported as the mean of at least three experiments ±S.E.

RESULTS

The role of Ca^{2+} in the catalytic activity of cABC I toward CS and DS substrates was investigated in a systematic fashion. First, the effect of Ca^{2+} and other divalent metal ions on the specific activity of the enzyme was measured. Second, the direct binding of Ca^{2+} to the enzyme was investigated by titration with terbium, a calcium analogue. Third, the effects of Ca^{2+} on the chemical kinetics of CS and DS substrate processing were measured. Finally, the molecular basis for the role of Ca^{2+} in substrate processing was investigated in detail using theoretical enzyme−substrate complexes and site-directed mutagenesis studies.

Chondroitinase ABC I Activity Analysis. The effect of various divalent ions on the activity of cABC I against C6S and DS substrates was assessed (Table 1). With C6S as the substrate, there was no apparent change in enzyme activity upon the addition of calcium or magnesium. There was a slight reduction in activity on addition of manganese. The addition of zinc appeared to have an inhibitory effect, as reported previously (*30*, *31*). Interestingly, the activity of cABC I on DS increased dramatically in the presence of added calcium or magnesium compared to that of the control (1 mg/mL DS in 50 mM Tris at pH 8.0). Manganese had no appreciable effect on DS depolymerization. The addition of zinc shows a minor (2-fold) but significant increase in the processing of DS.

In order to further understand the role of calcium in the selective enhancement of cABC I activity toward DS, we first sought to evaluate the calcium concentration at which maximal activity was observed. For these calcium titration experiments, an experimental arrangement based on the rate of product formation was employed, and the concentration of added $CaCl_2$ was varied from 0−40 mM. The data clearly

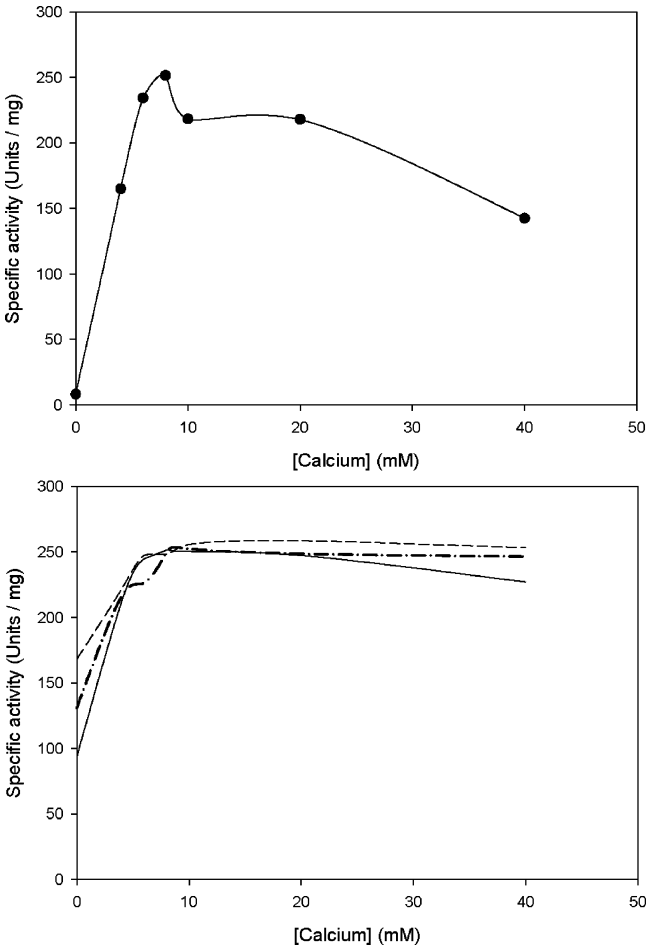

FIGURE 1: Effects of Ca^{2+} on the cABC I-mediated processing of dermatan sulfate. Calcium enhances the specific activity of cABC I acting on dermatan sulfate as a substrate. Briefly, activity was measured by tracking the formation of product as the absorbance at 232 nm on a spectrophotometric platform, where 0.2 μg of recombinant cABC I enzyme was placed in reaction with 1 mg/mL DS at each $CaCl_2$ concentration. (A) Effect of calcium on the activity of cABC I cleaving DS in the absence of any added sodium acetate. (B) Effect of calcium on the cABC I-mediated depolymerization of DS in the presence of added sodium acetate (25 mM, solid line; 50 mM, long dashed line; 100 mM, short dashed line).

indicated that maximum activity was obtained at ~10 mM $CaCl_2$ (Figure 1A).

It is important to note that our initial experiments with added calcium were done in the absence of any additional salt in the buffer; therefore, we next set out to ascertain whether the enhancement observed for DS processing was dependent on the presence of the divalent ions or was simply a byproduct of a salt effect. To this end, we performed a comparison of the activity of the enzyme on DS in the presence of set quantities of sodium acetate (*23*) over a range of calcium concentrations. Dermatan sulfate at a 1 mg/mL concentration was dissolved in 50 mM Tris buffer at pH 8.0 containing 25 mM, 50 mM, or 100 mM sodium acetate. Using each of these as our starting solutions, we repeated the calcium titration analysis by adding various amounts of $CaCl_2$ (0−20 mM). As illustrated in Figure 1B, the rate of enhancement observed upon the addition of 10 mM $CaCl_2$ still exceeds that observed when using the optimum salt concentration (100 mM sodium acetate). The results also indicate that the maximum enhancement observed is constant at 10 mM calcium, irrespective of the sodium acetate content in the starting buffer. These studies resolve the competing effects of salt and calcium on the cABC I-mediated depolymerization of DS, and are an indication that the effect of calcium is independent of a salt effect.

Interaction of Terbium with cABC I. In order to address whether cABC I itself binds calcium, we studied the interaction of Tb^{3+} with the recombinant enzyme in the absence of substrate. This experimental design allows for the assessment of cABC I-terbium interactions independently, that is, without the confounding factors associated with terbium−substrate interactions. Tb^{3+} is a lanthanide analogue of calcium, often used to probe the nature of protein interactions with divalent ions including calcium (*32*). In aqueous solution, Tb^{3+} possesses an ionic radius that is very similar to that of calcium. Another beneficial attribute of the protein−Tb^{3+} complex is that it is fluorescent. The increased charge properties of terbium compared to those of calcium additionally confer a relatively greater affinity to calcium-binding sites for the lanthanide than for the divalent calcium.

Upon titration of cABC I with terbium, an increase in fluorescence was observed against both a direct excitation of the terbium adduct (488 nm) and at an excitation of the proximal tyrosine side chains, which results in an energy transfer to the terbium adduct (280 nm). Fluorescence intensity increased upon terbium titration to cABC I until a terbium concentration of 8 mM (Figure 2A). The fluorescence intensity plateaued at this concentration and did not respond to further terbium addition.

Terbium often binds with greater affinity to a given site than does calcium. Therefore, an excess of calcium is likely required in order to displace terbium from binding sites within a terbium−enzyme complex. Such a competition between terbium and calcium for a position within the enzyme active site is useful for the purpose of inspecting the specificity of binding interactions. In an attempt to occupy enzyme binding sites, the enzyme was pre-loaded with 6 mM terbium. Calcium was added to the terbium/enzyme solution, and the fluorescence was measured. As shown in Figure 2B, the addition of calcium does effectively compete with terbium to occupy cABC I binding positions. These results indicate that the interaction of terbium with cABC I is specific and that this interaction substitutes for calcium binding to cABC I. These results are consistent with previous experiments on heparinase I designed to establish terbium−enzyme interaction and calcium specificity (*26*).

Calcium Increases Dermatan Sulfate Processing by cABC I. To further confirm the substrate-selective rate enhancement in the presence of calcium, we undertook a kinetic analysis of cABC I processing on C6S and DS in the presence and absence of 10 mM calcium chloride. The results are summarized in Table 2. With C6S as the substrate, the presence of 10 mM calcium had no effect on either the K_m or k_{cat} of the enzyme. The presence of calcium, however, clearly had an effect on the activity of cABC I when DS was the substrate. We observe an effective doubling of the turnover (k_{cat}) from 17 000 min^{-1} to 33 000 min^{-1} in the presence of calcium. The K_m was 1.4 μM in the absence of calcium and 2.9 μM in the presence of calcium. This suggests that calcium is possibly involved in the binding and orientation of the dermatan substrate in the active site. These

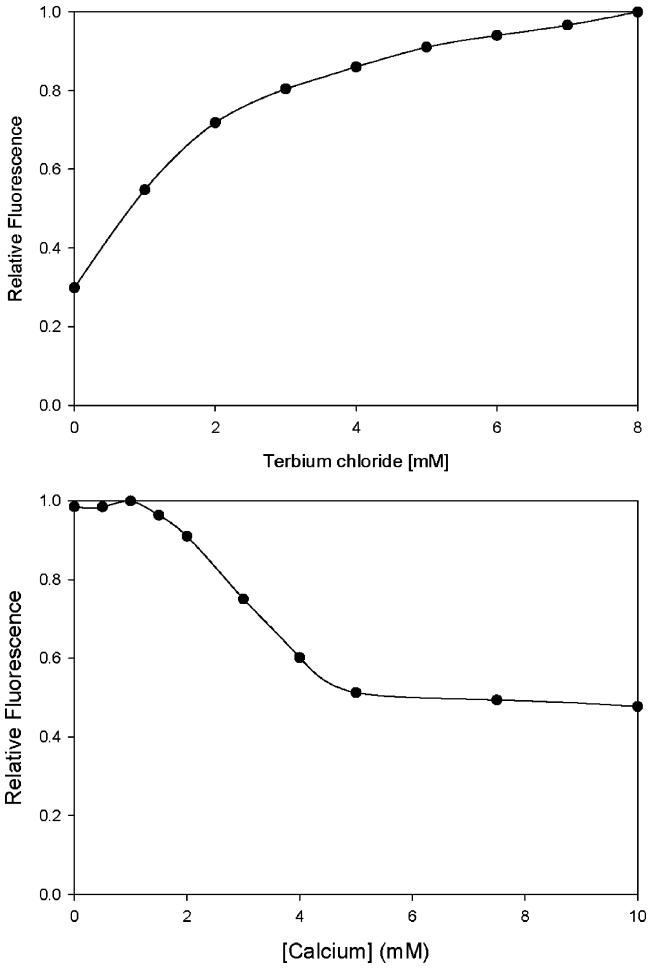

FIGURE 2: Biophysical characterization of cABC I interactions. Fluorescence spectrometry was used to assess the nature of ion binding to cABC I. The interaction of terbium, a fluorescent analogue of calcium, with the enzyme was observed against a direct excitation of the terbium adduct and at excitation of proximal tyrosine residues (488 and 280 nm, respectively). (A) Terbium binding to cABC I was investigated. Fluorescence intensity increases upon titration of terbium to 5 μM cABC I. Following the addition of $TbCl_3$, the solution was allowed to come to equilibrium, and the fluorescence at 545 nm was measured with an excitation wavelength of 280 nm. The data is presented as relative fluorescence normalized according to the peak measurement vs supplemented terbium. (B) Experiments were performed to investigate whether calcium was capable of competing for cABC I binding sites with terbium. The terbium−enzyme complex (6 mM terbium) was titrated with increasing amounts of calcium. The sample was incubated for 15 min, and the fluorescence at 545 nm was measured. Fluorescence intensity decreased with increased calcium concentration. Relative fluorescence is presented in normalized form according to the peak fluorescence measured.

phenomena provide an optimal conformation between substrate and enzyme that facilitates more rapid processing. It further offers an additional level of control regarding specificity, in that it can compromise the binding affinity of the substrate for the enzyme.

In our previously derived theoretical models of the enzyme−substrate structural complexes, we observed that in the case of CS, both the *C*-5 proton and the glycosidic oxygen in the cleavable linkage face the active site, whereas in the case of the DS substrate, these atoms are oriented in opposite directions (*24*). On the basis of these observations, we had proposed that the DS substrate could potentially

Table 2: Kinetic Analysis of Chondroitinase ABC I Acting on Chondroitin-6-sulfate and Dermatan Sulfate in the Presence of Calcium[a]

experiment	K_m (μM)	k_{cat} (min^{-1})	k_{cat}/K_m ($\mu M^{-1} min^{-1}$)
substrate: chondroitin-6-sulfate			
buffer only[b]	2.4 ± 0.9	22000 ± 1200	9100
buffer + 10 mM $CaCl_2$	2.9 ± 0.6	20000 ± 5000	6900
substrate: dermatan sulfate			
buffer only	1.4 ± 0.5	17000 ± 1400	12000
buffer + 10 mM $CaCl_2$	2.9 ± 0.5	33000 ± 1800	11000

[a] Recombinant cABC I (1 μL of 0.2 μg/μL enzyme) was added to 249 μL of a solution containing the substrate (0.1 to 5.0 mg/mL C6S or DS) in 50 mM Tris-HCl and 50 mM sodium acetate at pH 8.0 in either the presence or the absence of 10 mM calcium chloride. Product formation was monitored by measuring the absorbance at 232 nm every 2 s. The values are the mean of at least three experiments ±S.E. [b] The buffer is 50 mM Tris-HCl and 50 mM sodium acetate at pH 8.0

reorient itself through a slight rotation to facilitate both proton abstraction and protonation of the leaving group by the catalytic amino acids. Given the differential effect of calcium in enhancing DS processing, it is likely that calcium plays a role in establishing the proper DS orientation by binding to both substrate and enzyme. It is in this element that the differential processing of GAG substrates by cABC I manifests. These molecular aspects were investigated by further examining the enzyme−substrate complexes derived from our previous study (*24*).

Calcium Coordination Site. Divalent cations have historically been demonstrated to play a critical role in the enzymatic depolymerization of IdoA-containing GAGs. In the case of heparinase I, which predominantly cleaves GlcNS,6S−IdoA2S linkages in heparan sulfate GAGs, two Ca^{2+} binding sites were identified, where one was implicated in substrate binding and the other in the catalytic mechanism (*25*). More recently, a crystal structure of cB (an enzyme that cleaves DS as its sole substrate) with enzymatic degradation products revealed the presence of a Ca^{2+} ion in the active site (*27*). This crystal structure demonstrated that the conformational flexibility of IdoA enhanced the structural fit of the DS substrate into the active site and that the Ca^{2+} ion facilitated these interactions by coordinating both with the active site amino acids as well as the carboxylate group of the IdoA in the substrate. This provided a structural basis for the ability of cB to selectively cleave IdoA-containing DS substrates in comparison with GlcA-containing CS substrates (*27*).

Because cABC I cleaves both CS and DS substrates, it provided an interesting system to study the preferential effect of Ca^{2+} in processing these substrates. The crystal structure of cABC I provided a unique framework to understand the potential differences in the catalytic processing of GlcA-containing CS substrates and IdoA-containing DS substrates by this enzyme. By docking tetrasaccharide CS and DS substrates into the putative active site of cABC I, we obtained some preliminary structural insights into the differences in the processing of these substrates (*24*). Importantly, these differences were attributed to the relative orientation of the *C*-5 proton of the uronic acid in the +1 subsite and the oxygen atom in the cleavable glycosidic linkage. Whereas in GlcA-containing CS substrates, both of these atoms were facing in the same direction toward the putative active site

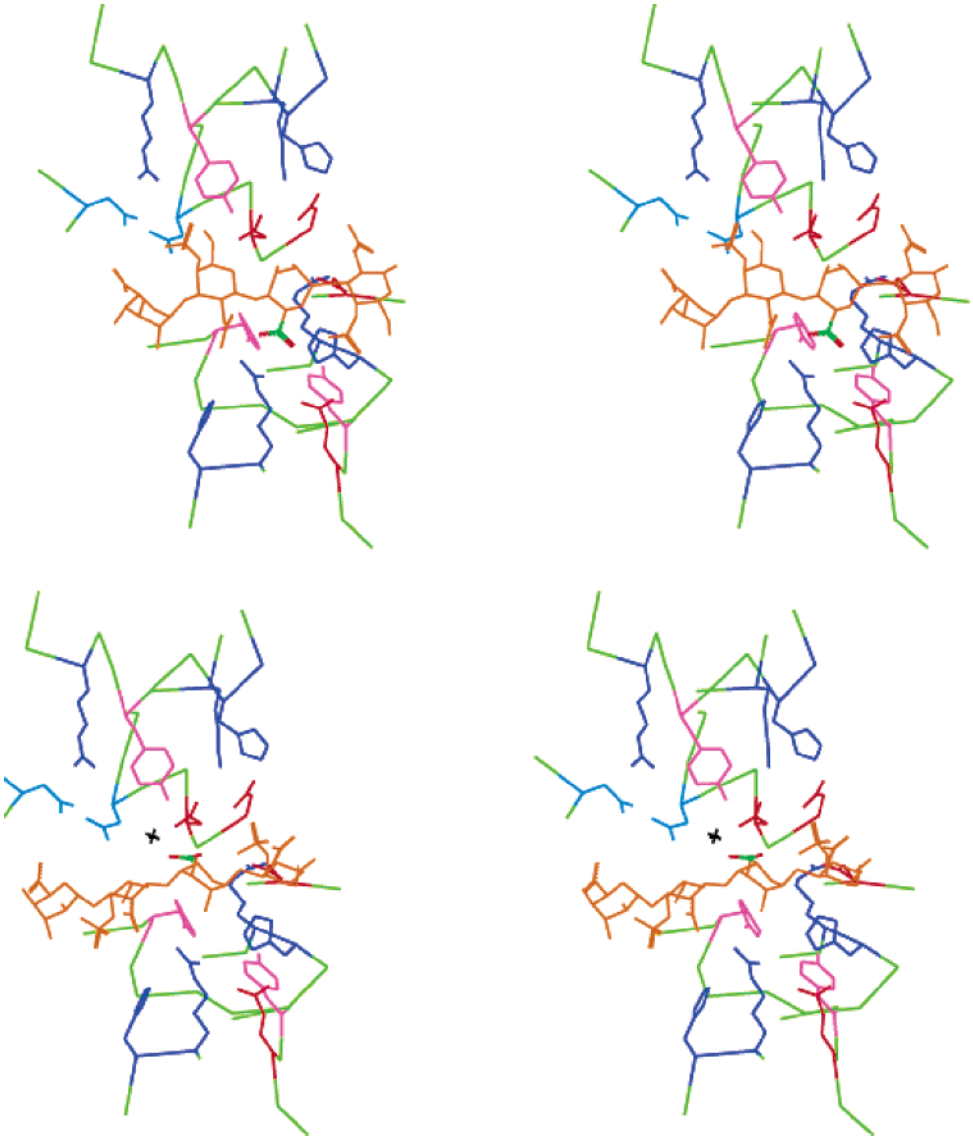

FIGURE 3: Role of Ca^{2+} in the processing of DS substrates by cABC I. Top: the stereo representation of the active site of cABC I with a docked dermatan sulfate substrate (*24*). Bottom: the stereoview of the potential reorientation of the DS substrate in the active site of cABC I. This reorientation of the DS substrate, which is stabilized by Ca^{2+} binding, improves the activity of cABC I toward DS. On the basis of the positioning of the oxygen atoms, the likely location of the Ca^{2+} ion is indicated by a black x. The carboxyl oxygens of Asp444 and the IdoA in the +1 subsite are positioned to coordinate with the Ca^{2+} ion in the active site. The CA trace is represented in green; the sidechains shown in the active site are Lys, His, and Arg in blue; Tyr in purple; Asp and Glu in red; and Asn and Gln in cyan. The dermatan substrate is colored gold, whereas the carboxyl group of the IdoA in the +1 subsite is colored differently (carbon atom in green and oxygen atoms in red) to highlight the change in orientation of the DS substrate in the top schematic compared to that in the bottom schematic.

residues, in the case of IdoA-containing DS substrates, they were facing in opposite directions (one toward the active site and the other away from the active site). On the basis of this observation, we proposed that the DS substrate could potentially undergo conformational change during catalysis such that both the *C*-5 proton abstraction and the protonation of the leaving anomeric oxygen atom (the glycosidic oxygen prior to cleavage) would be accomplished at the catalytic site.

In this study, further investigations into the theoretical models of the enzyme−substrate complexes revealed four aspartic acid residues, Asp439, Asp442, Asp444, and Asp490, which could potentially be involved in Ca^{2+} coordination. Among these residues, Asp444 was the closest to the active site. Building on our earlier studies, we sought to investigate whether the processing of DS by cABC I would involve a conformational change in the substrate which could be stabilized by interaction of Ca^{2+} with the substrate as well as the enzyme in the active site. In our previous study, we docked the DS substrate into the active site such that the *C*-5 proton of the IdoA in the +1 subsite was facing the active site. Using a similar approach as that outlined in our previous study (*24*), we docked the same DS substrate such that the glycosidic oxygen atom of the cleavable linkage was facing the active site (Figure 3). In this substrate conformation, the carboxylate group of the IdoA in the +1 subsite faces the Asp444 residue, thus indicating the potential coordination site for Ca^{2+} involving the oxygen atoms of Asp444 and those of the carboxylate group of the IdoA in the substrate (Figure 4). Apart from the four oxygen atoms of Asp444 and the IdoA, the oxygen atoms of Tyr392 and Asn447 are positioned such that they could also be involved

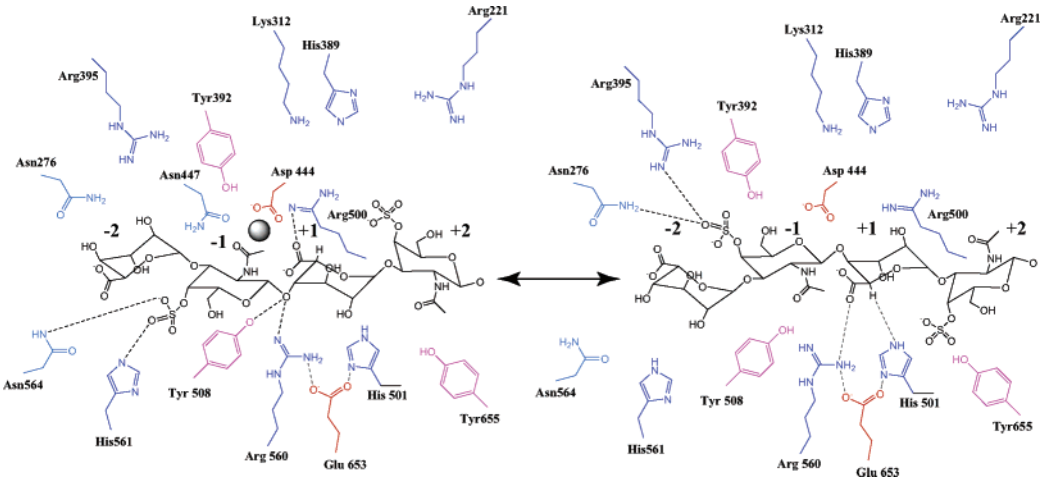

FIGURE 4: Schematic of DS substrate reorientation stabilized by Ca^{2+} binding. Right: a schematic of the DS substrate in the active site, where the *C*-5 proton of the IdoA in the +1 subsite is positioned to be abstracted by His501. Left: a schematic of the proposed reorientation of the DS substrate in the active site, where the glycosidic oxygen atom at the −1/+1 linkage is positioned to be protonated by Tyr508 or Arg560. This orientation of the substrate is stabilized by Ca^{2+} coordination in the active site. This appears to most likely involve the carboxyl oxygens of the IdoA in the +1 subsite, Asp444, and the oxygen atom of either Tyr392 or Asn447, or both.

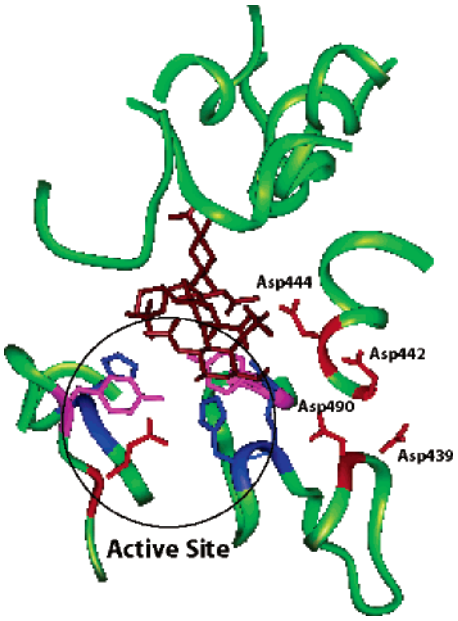

FIGURE 5: Active site topology of the cABC I active site. A GAG (maroon) substrate is shown in the catalytic cleft of cABC I (backbone in green) in close proximity to the active site residues (sequestered within circle) and several aspartic acid residues. Residues Asp439, Asp442, Asp444, and Asp490 were examined through mutagenesis studies in order to inspect their potential complicity within a calcium coordination center.

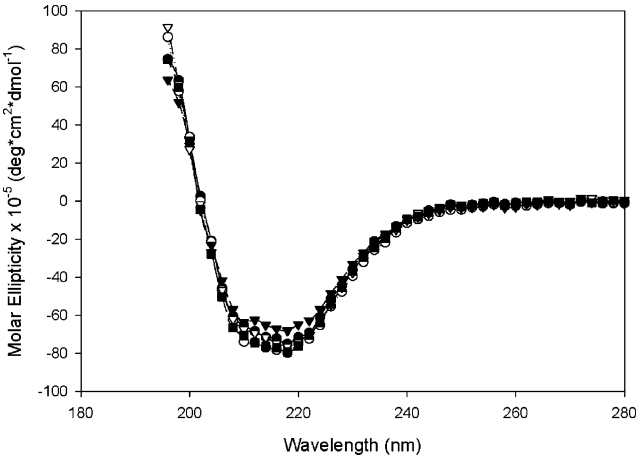

FIGURE 6: CD spectra of cABC I and mutants. The recombinant cABC I (●) and the mutants Asp442Ala (○), Asp439Ala (▼), Asp444Ala (▽), and Asp490Ala (■) were examined via circular dichroism spectroscopy to inspect potential alterations to protein structure following mutagenesis. The proteins were concentrated and buffer-exchanged into 50 mM sodium phosphate buffer at pH 8.0. Proteins were analyzed in a quartz cell with a 0.1 cm path length. All spectra were collected using a protein concentration of 0.2 mg/mL. CD spectra were recorded between 195 and 280 nm, averaging three scans per spectra. The CD signals were normalized to molar ellipticity.

in interacting with the Ca^{2+} ion. Furthermore, the theoretical enzyme−substrate model also provides a plausible explanation for the selective dependence of cABC I processing of the DS substrate on the Ca^{2+} ion concentration as observed in the kinetic studies.

Calcium Coordination Mutagenesis Studies. Site-directed mutagenesis studies were employed to further inspect the role calcium might play in the cABC I-mediated depolymerization of GAG substrates. On the basis of our model of the cABC I−dermatan structural complex, four aspartic acid residues, Asp439, Asp442, Asp444, and Asp490, were chosen as potential players in the coordination of divalent ions (Figure 5). Tyr392 was further inspected, as our model suggested its oxygen atoms may interact with a calcium ion. These residues were each independently mutated to alanine. To confirm that mutagenesis did not compromise the structure of the mutant proteins, the secondary structure of the proteins was analyzed using circular dichroism spectroscopy (Figure 6).

Our structural model of the enzyme−substrate complex suggests a direct role in calcium coordination for the Asp442 and Asp444 residues, according to proximity to the dermatan IdoA; Asp439 is more distant and is unlikely to play a central role in divalent ion coupling. Table 3 summarizes the activity of the cABC I mutants against the C6S substrate in the absence and in the presence of 10 mM Ca^{2+}. Specific activity measurements of recombinant cABC I against the C6S substrate did not show a dependence on calcium (Table 1). This result is consistent according to the kinetic parameters of the wild-type enzyme (Table 2), where both the K_m and

Table 3: Chondroitin-6-sulfate Kinetic Analysis of Mutants: Ca^{2+} Effects[a]

mutant	±10 mM Ca^{2+}	K_m (μM)	k_{cat} (min^{-1})	k_{cat}/K_m ($\mu M^{-1} min^{-1}$)
Asp439Ala	−	1.5 ± 0.7	3300 ± 1300	2200
Asp439Ala	+	1.7 ± 0.7	4000 ± 1100	2400
Asp442Ala	−	4.0 ± 0.9	400 ± 200	100
Asp442Ala	+	4.5 ± 1.1	510 ± 240	110
Asp444Ala	±	n.d.[b]	n.d.	n.d.
Asp490Ala	−	17.7 ± 9.5	2100 ± 350	120
Asp490Ala	+	14.5 ± 1.9	1800 ± 400	120

[a] The activity of mutant enzymes against the C6S substrate was assessed as detailed earlier (Table 2 and Experimental Procedures). The values are the mean of at least three experiments ±S.E. [b] n.d., kinetic parameters not determined because of the low activity of the mutant.

Table 4: Dermatan Sulfate Kinetic Analysis of Mutants: Ca^{2+} Effects[a]

mutant	±10 mM Ca^{2+}	K_m (μM)	k_{cat} (min^{-1})	k_{cat}/K_m ($\mu M^{-1} min^{-1}$)
Asp439Ala	−	1.7 ± 0.7	2300 ± 90	1400
Asp439Ala	+	2.8 ± 0.3	4500 ± 340	1600
Asp442Ala	±	n.d .[b]	n.d.	n.d.
Asp444Ala	±	n.d.	n.d.	n.d.
Asp490Ala	−	12 ± 4.0	280 ± 90	19
Asp490Ala	+	19 ± 7.2	640 ± 80	34

[a] The activity of mutant enzymes against the DS substrate was assessed as detailed earlier (Table 2 and Experimental Procedures). The values are the mean of at least three experiments ±S.E. [b] n.d., kinetic parameters not determined because of the low activity of the mutant.

the turnover number are consistent with or without supplemented calcium. Kinetic analysis of the Asp439Ala mutant on C6S (Table 3) reveals reduced total activity compared to that of the wild-type enzyme but does not present any calcium-mediated alteration in binding (K_m of 1.5 μM in the absence of Ca^{2+} and 1.7 μM in the presence of Ca^{2+}), turnover (k_{cat} of 3300 min^{-1} vs 4000 min^{-1}), or catalytic efficiency (k_{cat}/K_m of 2200 μM^{-1} min^{-1} vs 2400 μM^{-1} min^{-1}). The Asp439Ala mutant does react differentially to supplemented calcium in a DS-based assay, with a virtual doubling in k_{cat} on addition of Ca^{2+}, further excluding this residue as a potential calcium coordination player (Table 4). The processing of the C6S substrate by the Asp442Ala and Asp490Ala mutants also did not result in altered kinetic rates according to the inclusion of calcium, though both catalyzed the degradation of C6S at far lower rates than the wild type (Tables 2 and 3). Asp444Ala had a very low activity, and thus, establishing kinetic parameters was not possible. This is likely the result of the proximity of this residue to the catalytic center (Figure 4), where perturbation of the active site microenvironment could substantially alter electrostatics or the binding of substrate, even in a situation where calcium coordination is not necessarily required (Figure 5).

As established earlier, the processing of DS by cABC I proceeds in a calcium-dependent manner (Table 2). Calcium is important for the optimal depolymerization of DS, as seen with the mutants Asp442Ala and Asp444Ala. Our attempts to collect kinetic data on the mutants Asp442Ala and Asp444Ala indicated that these mutants have negligible activity against DS (Table 4). These residues are both within coordination proximity to the cABC I active site and the IdoA carboxylate and are inactive against DS, irrespective of the presence of divalent ions. These results tend to suggest that Asp442 and Asp444 may be part of the calcium coordination site in cABC I and, thus, are essential for the optimal processing of DS. The Asp490Ala mutant, from which our enzyme−substrate structural model suggests an intermediate role in calcium coordination that is greater than that mediated by Asp439 but less central than Asp442 and Asp444, does show a k_{cat}-dependent activity. The presence of calcium does increase comparative turnover more than 2-fold for this mutant (k_{cat} in the absence of calcium is 280 min^{-1} and in the presence of calcium is 640 min^{-1}). The mutant Tyr392Ala, positioned according to our enzyme−substrate structural complex as potentially involved in calcium coordination, displayed a 7-fold greater activity on C6S (specific activity of 84 units/mg) processing versus that on DS (specific activity of 12 units/mg) processing. This ratio is important to note in the context of wild-type cABC I processing, in which DS processing is far more comparable to C6S depolymerization in our activity screens (Table 1). These results suggest some role for Tyr392 in the strategy employed by cABC I to cleave IdoA-containing GAGs.

DISCUSSION

Given the broad range of substrates amenable to cleavage by cABC I, this system presents both opportunities as well as challenges with respect to the molecular aspects of substrate binding and catalysis. Although the structural fold of this enzyme is similar to that of cAC, the substrate-binding groove is wider and is composed of numerous basic amino acids and tyrosines. Our initial biochemical characterization of cABC I enabled us to confirm the critical amino acids among these various candidates (*23*). Furthermore, the theoretical enzyme−substrate complexes constructed in these studies provided preliminary insights into the potential differences in the processing of CS and DS substrates by cABC I (*24*).

Herein, we build a case to further clarify the phenomena by which cABC I is able to differentially process CS and DS substrates. Our results from this study suggest a calcium coordination strategy that cABC I employs to optimally process DS substrates. We further suggest that this divalent ion incorporation is not required for the cABC I-mediated depolymerization of chondroitin substrates. These studies comprise the first evidence characterizing a dual-activity scaffold for a broad substrate specificity glycosaminoglycan-degrading enzyme, where catalysis of one class of substrates proceeds with a mechanism distinct from that used for other substrates.

Titration with calcium clearly increases the efficiency of cABC I-mediated DS degradation. Further biochemical and biophysical investigations confirm that cABC I binds calcium. Several residues proximal to the catalytic site, specifically Asp442, Asp444, and Tyr392, were shown to be critical to cABC I function against DS and are the most likely to be involved in calcium binding. It is challenging to conclusively determine the role of these amino acids in the calcium-mediated processing of DS substrates. This is primarily due to their proximity to the active site. Thus, the site-directed mutagenesis of these amino acids (particularly the two aspartates) has an overall negative effect on the catalytic activity of the enzyme. Nevertheless, on the basis of our understanding of other GAG lyases and the current

studies, we suggest a molecular mechanism involved in cABC I-mediated DS depolymerization.

In the context of the general β-elimination mechanism postulated for the lyase-based depolymerization of GAGs (*33*, *34*), a cation (such as calcium) is poised to interact with the carboxylate anion of the substrate. This in turn decreases the pK_a of the carbon acid to such a degree that the α-proton can be abstracted by a basic amino acid within the active site of the enzyme. A variety of enzymatic systems have been implicated to employ calcium-binding processes for catalysis. Most notably, these include trypsin (*35*), chondroitinase B (*27*), heparinase I (*25*, *26*), and pectate lyase C (*28*). In the case of the polysaccharide lyases such as chondroitinase B and pectate lyase C, it has been demonstrated that the substrate undergoes a conformational change during catalysis.

The overall conformation of GAGs is influenced by monovalent and divalent counter ions such as sodium and calcium. Furthermore, the ability of IdoA to adopt multiple ring conformations further enhances the conformational changes of the GAG chain induced by different metal ions. In the case of cB, the conformational flexibility of IdoA enhances the conformational changes in the DS substrate, which cause the substrate to bend into the active site, where it is involved in calcium coordination along with the enzyme (*27*). Similarly, the poly galacturonic acid backbone of the pectate substrate has been shown to undergo a transition from a 3_1 to a 2_1 helical symmetry during catalysis (*28*). The coordination with the calcium ion in the active site has been implicated to play a role in this conformational change of the pectate substrate.

A structural comparison of cABC I from *Proteus vulgaris* and cAC from *Pedobacter heparinus* indicates a similarity in overall architecture of the enzymes including the active site loci. This would tend to suggest that cABC I is actually more appropriately suited to cleaving those substrates favored by cAC, that is, CS. This is borne out by our earlier studies on cABC I, which indicate that cABC I processes CS substrates more favorably (from a kinetic standpoint) than DS substrates (*23*). Our modeling studies suggest that for CS substrates, the *C*-5 proton of the glucuronic acid moiety is properly situated for facile abstraction by cABC I active site residues. In the case of DS, this proton is situated far less favorably, distant from the relevant locus within the active site, suggesting that the DS substrate could potentially undergo conformational changes in the active site that facilitate the *C*-5 proton abstraction and protonation of the glycosidic oxygen by the same active site residues.

On the basis of the above rationale and our results in this study, we propose that a conformational change of the DS substrate in the active site is influenced by its coordination with the calcium ion. Such coordination would potentially involve the carboxyl group of iduronic acid and the amino acids in the active site. It is challenging to establish the exact sequence of steps that bring about this transition state (calcium coordination) complex involving the enzyme and the substrate. Efforts are ongoing to obtain cocrystal structures of cABC I with CS and DS substrates. These structures would provide additional structural insights into the calcium-mediated processing of DS substrates by cABC I.

Recombinant GAG-degrading lyases are being developed for their potential relevance to multiple systems. These include a variety of therapeutic indications (*20*, *36*, *37*) and analytical applications (*10*, *24*, *38*−*41*). In the context of cABC I, the studies described in this report are useful in a variety of ways. First, they more fully inform the technologist of the mechanistic details of this tool, specifically with regard to an understanding of the full spectrum of potential substrates. Additionally, they offer the possibility of divalent triggers, where broad substrate specificity enzymes might be manipulated to have a refined specificity, with temporal or spatial-sensitive tuning, to a controlled enzyme-mediated reaction. This potentially could be used as one part of a strategy to deconvolute, for example, the species present in a complex mixture of glycans within a biological sample.

ACKNOWLEDGMENT

We thank Professors K. Dane Wittrup and Barbara Imperiali for access to instrumentation, and Professor V. Sasisekharan and Drs. Karthik Viswanathan and Ganpan Gao for critical reading of the manuscript.

REFERENCES

1. Morgenstern, D. A., Asher, R. A., and Fawcett, J. W. (2002) Chondroitin sulphate proteoglycans in the CNS injury response, *Prog. Brain Res. 137*, 313−332.
2. Silbert, J. E., and Sugumaran, G. (2002) Biosynthesis of chondroitin/dermatan sulfate, *IUBMB Life 54*, 177−186.
3. Hardingham, T. E., and Fosang, A. J. (1992) Proteoglycans: many forms and many functions, *FASEB J. 6*, 861−870.
4. Margolis, R. K., and Margolis, R. U. (1993) Nervous tissue proteoglycans, *Experientia 49*, 429−446.
5. Carulli, D., Laabs, T., Geller, H. M., and Fawcett, J. W. (2005) Chondroitin sulfate proteoglycans in neural development and regeneration, *Curr. Opin. Neurobiol. 15*, 116−120.
6. Hascall, V. C., Majors, A. K., De La Motte, C. A., Evanko, S. P., Wang, A., Drazba, J. A., Strong, S. A., and Wight, T. N. (2004) Intracellular hyaluronan: a new frontier for inflammation? *Biochim. Biophys. Acta. 1673*, 3−12.
7. Linhardt, R. J., al-Hakim, A., Liu, J. A., Hoppensteadt, D., Mascellani, G., Bianchini, P., and Fareed, J. (1991) Structural features of dermatan sulfates and their relationship to anticoagulant and antithrombotic activities, *Biochem. Pharmacol. 42*, 1609−1619.
8. Tully, S. E., Mabon, R., Gama, C. I., Tsai, S. M., Liu, X., and Hsieh-Wilson, L. C. (2004) A chondroitin sulfate small molecule that stimulates neuronal growth, *J. Am. Chem. Soc. 126*, 7736−7737.
9. Ernst, S., Langer, R., Cooney, C. L., and Sasisekharan, R. (1995) Enzymatic degradation of glycosaminoglycans, *Crit. Rev. Biochem. Mol. Biol. 30*, 387−444.
10. Venkataraman, G., Shriver, Z., Raman, R., and Sasisekharan, R. (1999) Sequencing complex polysaccharides, *Science 286*, 537−542.
11. Sugahara, K., Mikami, T., Uyama, T., Mizuguchi, S., Nomura, K., and Kitagawa, H. (2003) Recent advances in the structural biology of chondroitin sulfate and dermatan sulfate, *Curr. Opin. Struct. Biol. 13*, 612−620.
12. Sasisekharan, R., Bulmer, M., Moremen, K. W., Cooney, C. L., and Langer, R. (1993) Cloning and expression of heparinase I gene from Flavobacterium heparinum, *Proc. Natl. Acad. Sci. U.S.A. 90*, 3660−3664.
13. Shriver, Z., Hu, Y., and Sasisekharan, R. (1998) Heparinase II from Flavobacterium heparinum. Role of histidine residues in enzymatic activity as probed by chemical modification and site-directed mutagenesis, *J. Biol. Chem. 273*, 10160−10167.
14. Shriver, Z., Hu, Y., Pojasek, K., and Sasisekharan, R. (1998) Heparinase II from Flavobacterium heparinum. Role of cysteine in enzymatic activity as probed by chemical modification and site-directed mutagenesis, *J. Biol. Chem. 273*, 22904−22912.
15. Godavarti, R., Davis, M., Venkataraman, G., Cooney, C., Langer, R., and Sasisekharan, R. (1996) Heparinase III from Flavobacterium heparinum: cloning and recombinant expression in Escherichia coli, *Biochem. Biophys. Res. Commun. 225*, 751−758.

16. Pojasek, K., Shriver, Z., Kiley, P., Venkataraman, G., and Sasisekharan, R. (2001) Recombinant expression, purification, and kinetic characterization of chondroitinase AC and chondroitinase B from Flavobacterium heparinum, *Biochem. Biophys. Res. Commun. 286*, 343−351.
17. Fethiere, J., Eggimann, B., and Cygler, M. (1999) Crystal structure of chondroitin AC lyase, a representative of a family of glycosaminoglycan degrading enzymes, *J. Mol. Biol. 288*, 635−647.
18. Huang, W., Matte, A., Li, Y., Kim, Y. S., Linhardt, R. J., Su, H., and Cygler, M. (1999) Crystal structure of chondroitinase B from Flavobacterium heparinum and its complex with a disaccharide product at 1.7 A resolution, *J. Mol. Biol. 294*, 1257−1269.
19. Huang, W., Boju, L., Tkalec, L., Su, H., Yang, H. O., Gunay, N. S., Linhardt, R. J., Kim, Y. S., Matte, A., and Cygler, M. (2001) Active site of chondroitin AC lyase revealed by the structure of enzyme-oligosaccharide complexes and mutagenesis, *Biochemistry 40*, 2359−2372.
20. Liu, D., Shriver, Z., Venkataraman, G., El Shabrawi, Y., and Sasisekharan, R. (2002) Tumor cell surface heparan sulfate as cryptic promoters or inhibitors of tumor growth and metastasis, *Proc. Natl. Acad. Sci. U.S.A. 99*, 568−573.
21. Shriver, Z., Raguram, S., and Sasisekharan, R. (2004) Glycomics: a pathway to a class of new and improved therapeutics, *Nat. Rev. Drug Discovery 3*, 863−873.
22. Huang, W., Lunin, V. V., Li, Y., Suzuki, S., Sugiura, N., Miyazono, H., and Cygler, M. (2003) Crystal structure of Proteus vulgaris chondroitin sulfate ABC lyase I at 1.9A resolution, *J. Mol. Biol. 328*, 623−634.
23. Prabhakar, V., Capila, I., Bosques, C. J., Pojasek, K., and Sasisekharan, R. (2005) Chondroitinase ABC I from Proteus vulgaris: cloning, recombinant expression and active site identification, *Biochem. J. 386*, 103−112.
24. Prabhakar, V., Raman, R., Capila, I., Bosques, C. J., Pojasek, K., and Sasisekharan, R. (2005) Biochemical characterization of the chondroitinase ABC I active site, *Biochem. J. 390*, 395−405.
25. Liu, D., Shriver, Z., Godavarti, R., Venkataraman, G., and Sasisekharan, R. (1999) The calcium-binding sites of heparinase I from Flavobacterium heparinum are essential for enzymatic activity, *J. Biol. Chem. 274*, 4089−4095.
26. Shriver, Z., Liu, D., Hu, Y., and Sasisekharan, R. (1999) Biochemical investigations and mapping of the calcium-binding sites of heparinase I from Flavobacterium heparinum, *J. Biol. Chem. 274*, 4082−4088.
27. Michel, G., Pojasek, K., Li, Y., Sulea, T., Linhardt, R. J., Raman, R., Prabhakar, V., Sasisekharan, R., and Cygler, M. (2004) The structure of chondroitin B lyase complexed with glycosaminoglycan oligosaccharides unravels a calcium-dependent catalytic machinery, *J. Biol. Chem. 279*, 32882−32896.
28. Herron, S. R., Scavetta, R. D., Garrett, M., Legner, M., and Jurnak, F. (2003) Characterization and implications of Ca2+ binding to pectate lyase C, *J. Biol. Chem. 278*, 12271−12277.
29. Chevalier, F., Lucas, R., Angulo, J., Martin-Lomas, M., and Nieto, P. M. (2004) The heparin-Ca(2+) interaction: the influence of the O-sulfation pattern on binding, *Carbohydr. Res. 339*, 975−983.
30. Hamai, A., Hashimoto, N., Mochizuki, H., Kato, F., Makiguchi, Y., Horie, K., and Suzuki, S. (1997) Two distinct chondroitin sulfate ABC lyases. An endoeliminase yielding tetrasaccharides and an exoeliminase preferentially acting on oligosaccharides, *J. Biol. Chem. 272*, 9123−9130.
31. Sato, N., Shimada, M., Nakajima, H., Oda, H., and Kimura, S. (1994) Cloning and expression in Escherichia coli of the gene encoding the Proteus vulgaris chondroitin ABC lyase, *Appl. Microbiol. Biotechnol. 41*, 39−46.
32. Martin, R. B., and Richardson, F. S. (1979) Lanthanides as probes for calcium in biological systems, *Q. Rev. Biophys. 12*, 181−209.
33. Gerlt, J. A., and Gassman, P. G. (1993) Understanding the rates of certain enzyme-catalyzed reactions: proton abstraction from carbon acids, acyl-transfer reactions, and displacement reactions of phosphodiesters, *Biochemistry 32*, 11943−11952.
34. Jedrzejas, M. J. (2000) Structural and functional comparison of polysaccharide-degrading enzymes, *Crit. Rev. Biochem. Mol. Biol. 35*, 221−251.
35. De Jersey, J., Lahue, R. S., and Martin, R. B. (1980) Terbium luminescence as a probe of the calcium binding site of trypsin and alpha-chymotrypsin, *Arch. Biochem. Biophys. 205*, 536−542.
36. Bradbury, E. J., Moon, L. D., Popat, R. J., King, V. R., Bennett, G. S., Patel, P. N., Fawcett, J. W., and McMahon, S. B. (2002) Chondroitinase ABC promotes functional recovery after spinal cord injury, *Nature 416*, 636−640.
37. Sanderson, R. D., Yang, Y., Suva, L. J., and Kelly, T. (2004) Heparan sulfate proteoglycans and heparanase−partners in osteolytic tumor growth and metastasis, *Matrix Biol. 23*, 341−352.
38. Pojasek, K., Raman, R., Kiley, P., Venkataraman, G., and Sasisekharan, R. (2002) Biochemical characterization of the chondroitinase B active site, *J. Biol. Chem. 277*, 31179−31186.
39. Shriver, Z., Sundaram, M., Venkataraman, G., Fareed, J., Linhardt, R., Biemann, K., and Sasisekharan, R. (2000) Cleavage of the antithrombin III binding site in heparin by heparinases and its implication in the generation of low molecular weight heparin, *Proc. Natl. Acad. Sci. U.S.A. 97*, 10365−10370.
40. Guerrini, M., Raman, R., Venkataraman, G., Torri, G., Sasisekharan, R., and Casu, B. (2002) A novel computational approach to integrate NMR spectroscopy and capillary electrophoresis for structure assignment of heparin and heparan sulfate oligosaccharides, *Glycobiology 12*, 713−719.
41. Plaas, A. H., West, L., Midura, R. J., and Hascall, V. C. (2001) Disaccharide composition of hyaluronan and chondroitin/dermatan sulfate. Analysis with fluorophore-assisted carbohydrate electrophoresis, *Methods Mol. Biol. 171*, 117−128.

BI0605484